# Effect of Proton Transfer on the Anionic and Cationic Pathways of Pyrimidine Photodimer Cleavage. A Computational Study

**Janusz Rak,**[†] **Alexander A. Voityuk, Maria-Elisabeth Michel-Beyerle, and Notker Rösch***

*Institut für Physikalische and Theoretische Chemie, Technische Universität München,*
*D-85747 Garching, Germany*

Proton exchange between pyrimidine photodimers and their environment may have a profound impact on DNA photorepair. On the basis of B3LYP/6-31G* and AM1 calculations, we present the first computational study of the influence of protonation and deprotonation on the splitting reactions of pyrimidine dimer ion radicals. While proton transfer from a complementary adenine to a Pyr<>Pyr anion is calculated to be endothermic and, therefore, is unlikely in DNA, protonation of the dimer anion is feasible in polar solution. Cleavage of both nonprotonated and protonated dimer anions is a two-step reaction where C5−C5′ bond splitting is followed by cleavage of the C6−C6′ bond. However, the calculated activation barriers for the splitting of the protonated species are considerably higher than those for the corresponding nonprotonated anion. Proton transfer from a pyrimidine dimer cation to adenine is found to be energetically favorable. The opening of the cyclobutane ring in the dimer cation and its deprotonated state proceeds in reverse order: the C6−C6′ bond is broken first, followed by splitting of the C5−C5′ bond. Although the splitting of the dimer cation is activationless, rather high activation barriers are predicted for the cleavage of its deprotonated form in the gas phase. However, this barrier decreases substantially in a polar medium and, therefore, deprotonation of the dimer cation does not prevent its splitting in DNA nor in polar solution.

## Introduction

Hydrogen bonding plays a fundamental role in the structure and interaction of biomolecules.[1,2] Special attention has been paid to strong hydrogen bonds with regard to proton transfer.[3] When a strong hydrogen bond is formed between two systems, proton transfer from one molecule to the other may follow. Proton transfer is one of the most important features of enzymatic reactions; it may considerably affect the reaction mechanism in biological systems.[4] In the present study we will consider the possible role of proton transfer on the cycloreversion of cis−syn pyrimidine photodimers (Pyr<>Pyr).

These dimers are the most common lesions induced in DNA by UV radiation.[5] They are formed by photocycloaddition between pyrimidine bases which are adjacently located at the same DNA strand. In a wide range of living organisms there exist enzymes, DNA photolyases, which are able to repair these damages using the energy of visible light (350−500 nm).[5] Photolyases are assumed to mediate electron transfer from a cofactor, a reduced flavin in its excited singlet state, to Pyr<>Pyr, thereby initiating cleavage of the pyrimidine dimer.[3] As recently shown, pyrimidine dimer splitting can also result from electron transfer from Pyr<>Pyr to a metal complex in an excited state.[6] Thus, photorepair can in principle proceed via two different pathways: anionic and cationic. Both pathways have been studied in a number of experiments where cleavage of pyrimidine dimers was induced by photoreducing or photo-oxidizing agents.[7−9]

The dimer anion or cation radicals formed due to electron transfer to or from Pyr<>Pyr are found to be unstable. Recent theoretical studies showed that the kinetic barriers for the nonconcerted splitting of the dimer anions or cations are substantially lower than those for a neutral pyrimidine dimer.[10−14] In line with experiments, these findings suggest that Pyr<>Pyr should cleave almost immediately after electron transfer. However, an important question has not yet been discussed: Can proton exchange between the pyrimidine dimer ions and their environment inhibit the splitting process? Indeed, the positive charge on a dimer radical cation may be neutralized by proton transfer from the cation to a proton acceptor. Similarly, proton transfer to the dimer anion results in a neutral dimer radical. Proton exchange may affect the reactivity of the dimer ion radicals. The main goal of the present work is to study the importance of this effect.

Hydrogen bonds are an important prerequisite for proton transfer between a photodimer and an adjacent adenine base. Formation of a photodimer in DNA essentially leaves hydrogen bonds between thymine and the complementary base adenine unaffected.[15] In the cation Pyr<>Pyr[+], proton exchange between center N3 of the dimer and center N1 of adenine is conceivable (see Figure 1).[16,17] In the anion Pyr<>Pyr[−], proton transfer may occur in the opposite direction, from N6 of adenine to O4 of the dimer. Moreover, protonation/deprotonation of the charged model dimers may influence their cleavage in solution. Thus, it seems interesting to investigate the effect of proton transfer on the opening of the cyclobutane ring in Pyr<>Pyr ion radicals. In this work we have considered the following issues: (i) thermodynamic aspects of proton transfer between Pyr<>Pyr anions or cations and various proton donor or acceptor groups; (ii) the thermodynamic and kinetic stability of the neutral radical species formed after protonation of the dimer anion or deprotonation of the dimer cation; (iii) similarity and difference in the reaction behavior of these radical intermediates.

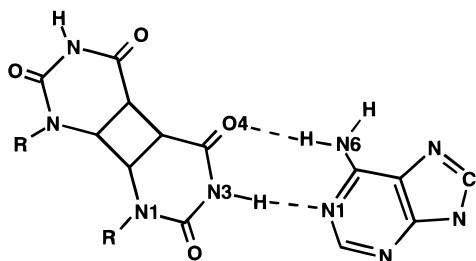† On leave from the Department of Chemistry, University of Gdansk, Sobieskiego 18, 80-952 Gdansk, Poland.

**Figure 1.** Hydrogen bonding between a uracil photodimer and complementary adenine in DNA.

## Methods

A uracil dimer in its cis−syn configuration (U<>U) was used in the present study. This model system comprises all important structural features of the biologically relevant thymine dimer T<>T, e.g., the puckering of the cyclobutane-type ring. However, because U<>U lacks two methyl groups compared to T<>T, it is less demanding from a computational point of view.

To describe the splitting process, we used both density functional (DF) calculations[18] and the semiempirical AM1 method.[19,20] The DF calculations (within the 6-31G* basis set[21]) employed Becke's three-parameter hybrid functional approach[22,23] in combination with the correlation functional of Lee, Yang, and Parr[24] (B3LYP). An assessment[25] of DF methods concludes that the B3LYP scheme provides the most reliable approach for determining structure and energetics of organic molecules. In a recent computational study[13] on the splitting of a uracil dimer cation we showed that the B3LYP/6-31G* level of theory is able to account for essential dynamical correlation effects.

Recently, it was shown for several small molecules that the so-called self-interaction error (SIE) may seriously affect the DFT energetics of radicals when current exchange-correlation approximations are used.[26,27] An especially large error may be expected for symmetric systems where separated fragments may have noninteger numbers of electrons; the SIE causes an artificial lowering of the energy of such systems. However, in the cases under investigation, a protonated dimer anion (PDA) or a depronated dimer cation (DDC), symmetry is broken because of protonation/deprotonation of one of the two uracil moieties. Therefore, the SIE should be rather small. Moreover, we estimated the possible SIE influence on the B3LYP results for a uracil dimer cation by single-point MP2 calculations on crucial structures.[14] Even for this system with (formally) two identical subunits, it was found that the stability of the complex relative to the separated monomers amounts to 31.7 kcal/mol at the B3LYP level and to 32.3 kcal/mol at MP2 level. The close agreement between B3LYP and MP2 results suggests that SIE is rather negligible for the present type of systems. Thus, we refrain from discussing any further the SIE of our results for the PDA and DDC splitting.[14]

No constraints were applied during geometry optimizations. Transition states were located employing the reaction coordinate method followed by gradient minimization. All stationary points were checked by a frequency analysis.[28]

The semiempirical AM1 method was used to estimate the influence of solvent effects on the cleavage reaction; an equivalent approach at the B3LYP/6-31G* level is much more time-consuming. To evaluate the influence of a polar environment (water) on thermodynamic and kinetic characteristics we employed the self-consistent reaction field approach.[29] AM1 calculations were also performed to select the lowest energy

isomers of protonated/deprotonated dimers which were subsequently modeled within the DF approach.

## Results and Discussion

**Model Selection and Thermodynamics of Proton Transfer.** Before studying how protonation of the photodimer anion or deprotonation of the dimer cation may affect the dimer splitting, we shall discuss the thermodynamics of the proton transfer between uracil dimer ion radicals and their environment. Because the biologically relevant reaction proceeds in DNA, we considered proton exchange between the dimer ions and an adenine base (see Figure 1). The splitting reaction was also experimentally studied in solution;[5,7,8] therefore, we also considered the thermodynamics of proton transfer for systems which include $H_3O^+/H_2O/OH^-$ and $H_3PO_4/H_2PO_4^-$.

The dimer ions exhibit several sites which may be involved in proton transfer. In particular, all oxygen atoms can be considered as proton acceptor sites. On the other hand, NH groups have amphoteric character. Taking into account the puckered structure of the cyclobutane ring in the pyrimidine dimer,[30,31] one should formally consider twelve dimer configurations. A DF analysis of the potential energy surface with regard to these twelve configurations requires substantial computational resources. Therefore, we decided to first explore the relative stability of protonated and deprotonated species using the AM1 method. For the protonated dimer anion (PDA), the relative values of the heat of formation calculated in the gas phase yield the following series of protonation sites: O4, 0.0 kcal/mol; O2, 6.5 kcal/mol; U<>U(N1), 27.5 kcal/mol; and N3, 32.6 kcal/mol (see Figure 1). Thus, O4 is the most probable protonation site of the dimer anion. In turn, the deprotonated dimer cation (DDC) has two tautomers. According to AM1, the species with deprotonated N1 is 6.9 kcal/mol more stable than the structure with deprotonated N3. Because the position N1 of pyrimidine in DNA is bound to the backbone chain it does not carry a proton. Moreover, in model systems experimentally studied in solution, the proton at N1 was substituted by alkyl groups.[7,8] Therefore, despite the energy argument in favor of N1 deprotonation, the center N3 of the dimer cation was considered as the deprotonation site.

The arrangement of hydrogen bonds in DNA suggests a further important argument for considering O4 and N3 of the dimer as sites involved in proton-transfer reactions (Figure 1). Thus, both hydrogen bonding in DNA and energy arguments lead to the conclusion that sites O4 and N3 of the dimer should be relevant to proton exchange.

Because the cyclobutane ring of the dimer has a puckered structure[30,31] additional geometry optimizations were carried out at the HF/6-31G* level to decide which of the two pyrimidines is responsible for proton exchange. We found that protonation/deprotonation of the primed pyrimidine ring (Figure 2) is energetically more favorable. In particular, DDC(N3′) and PDA-(O4′) turned out to be more stable by 0.6 and 1.6 kcal/mol, respectively, than the corresponding (unprimed) tautomers. Thus, the structures DDC(N3′) and PDA(O4′) (see Figure 2) were taken to model the splitting process at the B3LYP/6-31G* level.

We now the turn to a discussion of the energetics of proton transfer. The calculated energies of dimer ion radicals involved in proton exchange are collected in Table 1. At the B3LYP level, proton transfer from adenine to U<>U$^-$ is endothermic by 17 kcal/mol. Taking into account the solvent effect as estimated by AM1, one expects a reaction energy of about 15.8 kcal/mol. Note that the free energy of proton transfer between a thymine anion radical and an adenine molecule was experimentally
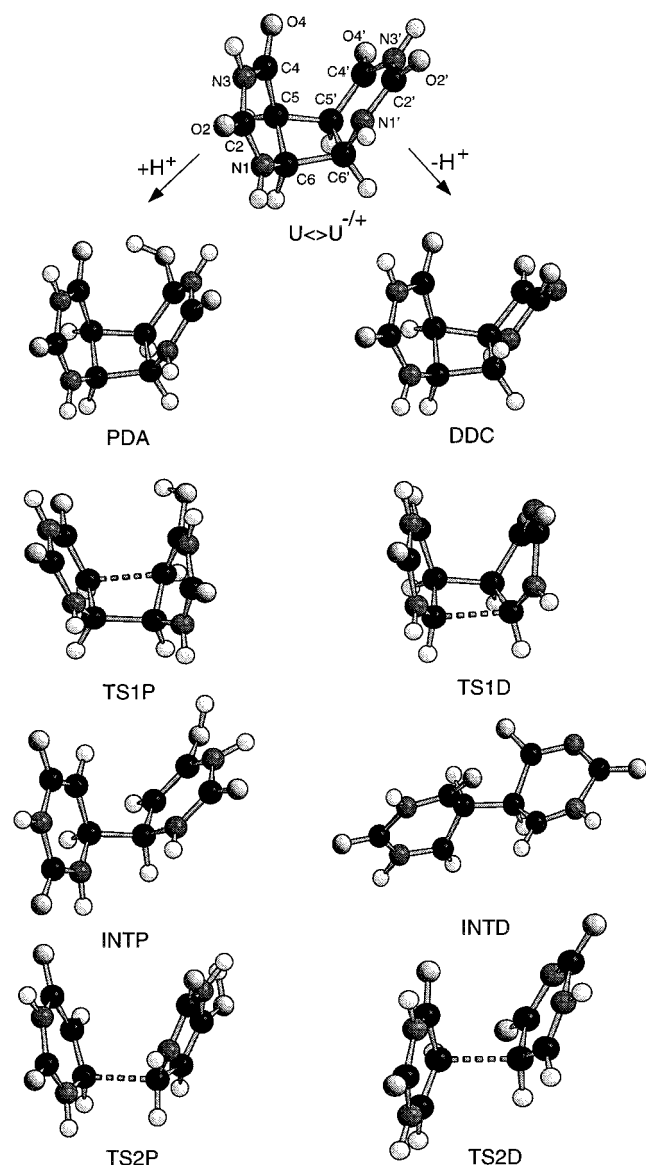
Computational Analysis of Proton Transfer

*J. Phys. Chem. A, Vol. 103, No. 18, 1999* **3571**



**Figure 2.** Structures of a protonated pyrimidine dimer anion radical (PDA) and a deprotonated pyrimidine dimer cation radical (DDC) as well as of related species formed during dimer cleavage calculated at the B3LYP/6-31G* level: U<>U$^+$ and U<>U$^-$, nonrelaxed geometries of a uracil dimer cation or anion; TS1P, transition state for the splitting of the first bond in PDA; INTP, PDA intermediate; TS2P, transition state for the splitting of the second bond in PDA; TS1D, transition state for the splitting of the first bond in DDC; INTD, DDC intermediate; TS2D, transition state for the splitting of the second bond in DDC.

estimated to be larger than 9.3 kcal/mol.[16,17] The situation for the dimer cation is quite different. In the gas phase, the deprotonation of U<>U$^+$ by adenine is exothermic, by $-11.4$ kcal/mol (B3LYP; Table 1). Solvation in a polar medium strongly reduces the reaction energy, to $-1.1$ kcal/mol. For comparison, note that the experimental free energy of proton transfer between a thymine cation radical and adenine is $-0.2$ kcal/mol.[16,32] Thus, proton transfer seems to occur in DNA during the splitting of a pyrimidine dimer cation, but it is rather improbable in the case of the dimer anion.

Although proton exchange involving the dimer anion seems to be inhibited in DNA, it may become feasible in the presence of proton donors that are stronger than adenine, e.g., in experimental studies in solution.[9] The results of Table 1 indicate that both phosphoric acid $H_3PO_4$ and $H_3O^+$ ions will induce

**TABLE 1: Deprotonation Enthalpy of a Uracil Dimer Cation Radical and Protonation Enthalpy of a Uracil Dimer Anion Radical in the Gas Phase and in Aqueous Solution (in kcal/mol)**

| | gas phase | | water | |
|---|---|---|---|---|
| reaction | B3LYP[a] | AM1 | B3LYP[b] | AM1 |
| U<>U$^+$ + $H_2O$ → DDC + $H_3O^+$ | 49.8 | 35.7 | 15.8 | 1.7 |
| U<>U$^+$ + $H_2PO_4$- → DDC + $H_3PO_4$ | $-103.0$ | $-131.5$ | 4.4 | $-24.1$ |
| U<>U$^+$ + Ade → DDC + Ade(+H)$^+$ | $-11.4$ | $-22.1$ | $-1.1$ | $-11.8$ |
| U<>U$^+$ + OH$^-$ → DDC + $H_2O$ | $-206.3$ | $-212.3$ | $-41.0$ | $-47.0$ |
| U<>U$^-$ + $H_2O$ → PDA + OH$^-$ | 76.1 | 63.1 | 35.0 | 22.0 |
| U<>U$^-$ + $H_3O^+$ → PDA + $H_2O$ | $-180.1$ | $-184.9$ | $-21.9$ | $-26.7$ |
| U<>U$^-$ + Ade → PDA + Ade($-$H)$^-$ | 17.0 | 2.2 | 15.8 | 1.0 |
| U<>U$^-$ + $H_3PO_4$ → PDA + $H_2PO_4$- | $-27.3$ | $-17.7$ | $-10.5$ | $-0.9$ |

[a] Reaction energy. [b] Solvent effect estimated from AM1 results.

**TABLE 2: Structural Parameters of the Protonated Pyrimidine Dimer Anion Radical and Related Species Resulting from the Dimer Splitting (see Figure 2) Calculated at the B3LYP/6-31G* Level (distances in Å, Angles in Degrees)**

| | U<>U$^-$ | PDA | TS1P | INTP | TS2P |
|---|---|---|---|---|---|
| bond distances[a] | | | | | |
| C6$-$N1 | 1.437 | 1.440 | 1.451 | 1.459 | 1.414 |
| C6′$-$N1′ | 1.448 | 1.445 | 1.449 | 1.457 | 1.412 |
| C4$-$O4 | 1.215 | 1.227 | 1.232 | 1.228 | 1.227 |
| C4′$-$O4′ | 1.214 | 1.366 | 1.354 | 1.362 | 1.357 |
| C5$-$C4 | 1.522 | 1.512 | 1.452 | 1.445 | 1.441 |
| C5′$-$C4′ | 1.517 | 1.484 | 1.391 | 1.340 | 1.352 |
| C5$-$C5′ | 1.567 | 1.591 | 2.021 | 3.073 | 3.246 |
| C6$-$C6′ | 1.572 | 1.580 | 1.582 | 1.578 | 2.045 |
| C5$-$C6 | 1.548 | 1.543 | 1.520 | 1.485 | 1.406 |
| C5′$-$C6′ | 1.550 | 1.554 | 1.533 | 1.499 | 1.447 |
| dihedral angles[a] | | | | | |
| H5$-$C5$-$C4$-$C6 | 130.7 | 131.4 | 154.5 | 179.3 | $-174.2$ |
| H5′$-$C5′$-$C4′$-$C6′ | $-126.7$ | $-127.8$ | $-150.3$ | 178.8 | 174.1 |
| H6$-$C6$-$N1$-$C5 | $-126.4$ | $-125.6$ | $-126.0$ | $-120.2$ | $-142.7$ |
| H6′$-$C6′$-$N1′$-$C5′ | 131.7 | 131.1 | 122.0 | 120.9 | 136.7 |
| C6′$-$C5′$-$C5$-$C6 | $-20.0$ | $-16.4$ | 13.9 | $-35.1$ | $-39.1$ |
| O4′$-$C4′$-$C5′$-$N3′ | 177.5 | $-146.1$ | $-174.5$ | 179.3 | 178.1 |

[a] For atom labeling see Figure 2.

protonation of a pyrimidine dimer anion in aqueous solution. The B3LYP reaction energies corrected for solvent effects amount to $-10.5$ and $-21.9$ kcal/mol, respectively. Hence, proton transfer from the environment to the dimer anion is energetically possible. A similar consideration for the dimer cation (Table 1) reveals that for reaction with OH$^-$ in water the equilibrium is shifted completely toward DDC (reaction energy is $-41.0$ kcal/mol). Thus, the splitting of both dimer cation and anion can be affected in solution by proton transfer.

**Structural Changes Accompanying the Cleavage of Protonated and Deprotonated Species.** Formally, the neutral radical PDA is obtained by adding a hydrogen atom at O4′ of U<>U. Similarly, DDC can be thought of as the result of hydrogen atom abstraction from N3′ of U<>U (see Figure 1 for the numbering of atoms). To answer the question how proton-transfer affects the dimer cleavage, one has to study the energy profile of the splitting of these neutral radicals PDA and DDC. Before discussing the energetics of these processes, let us consider the structural changes calculated for the transformations of these species. For assessing the cleavage reactions of both PDA and DDC, appropriate intermediates, transition states, and products have been calculated. In Figure 2 we display the structures of stationary points for the two reaction paths: 1A, splitting of the protonated dimer anion PDA; and 1B, splitting of deprotonated dimer cation DDC. Pertinent structural parameters, calculated at the B3LYP level, are collected in Tables 2 and 3 and compared to the structures of the corresponding ancestor ion radical dimers.

**TABLE 3: Structural Parameters of the Deprotonated Pyrimidine Dimer Cation Radical (DDC) and Related Species Resulting from the Dimer Splitting (see Figure 2) Calculated within B3LYP/6-31G\* (distances in Å, angles in degrees)**

| | $U<>U^+$ | DDC | TS1D | INTD | TS1D |
|---|---|---|---|---|---|
| bond distances[a] | | | | | |
| C6−N1 | 1.437 | 1.438 | 1.370 | 1.391 | 1.367 |
| C6′−N1′ | 1.448 | 1.446 | 1.328 | 1.282 | 1.309 |
| C4−N3 | 1.385 | 1.386 | 1.397 | 1.379 | 1.407 |
| C4′−N3′ | 1.386 | 1.402 | 1.355 | 1.354 | 1.354 |
| C5−C4 | 1.522 | 1.523 | 1.529 | 1.525 | 1.494 |
| C5′−C4′ | 1.517 | 1.533 | 1.568 | 1.584 | 1.538 |
| C5−C5′ | 1.567 | 1.566 | 1.573 | 1.537 | 1.997 |
| C6−C6′ | 1.572 | 1.570 | 2.075 | 3.394 | 3.468 |
| C5−C6 | 1.548 | 1.547 | 1.513 | 1.496 | 1.407 |
| C5′−C6′ | 1.550 | 1.552 | 1.520 | 1.484 | 1.425 |
| dihedral angles[a] | | | | | |
| H5−C5−C4−C6 | 130.7 | 130.6 | 125.1 | 119.5 | 141.9 |
| H5′−C5′−C4′−C6′ | −126.7 | −126.9 | −122.9 | −113.9 | −139.7 |
| H6−C6−N1−C5 | −126.4 | −126.8 | −149.5 | −150.5 | 173.9 |
| H6′−C6′−N1′−C5′ | 131.7 | 131.9 | 154.8 | 176.8 | −178.2 |
| C6′−C5′−C5−C6 | −20.0 | −20.1 | −14.9 | −91.2 | −83.2 |
| N3′−C4′−O4′−O2′ | −3.1 | −34.1 | 9.0 | −5.1 | −3.4 |

[a] For atom labeling see Figure 2.

Addition of a hydrogen atom to center O4 in PDA results in an elongation of the C4′−O4′ distance by 0.15 Å. Concomitant loss of sp[2] character at C4′ causes a considerable change of the dihedral angle O4′−C4′−C5′−N3′, from 177.5° in the neutral uracil dimer to −146.1° in PDA (Table 2). In addition, PDA is stabilized by the hydrogen bond O4···H4′···O4′ (see Figure 2); the distance O4···H4′ is calculated as 1.976 Å.

The cleavage reaction of PDA has two steps: formation of an intermediate INTP (Figure 2) after splitting of the bond C5−C5′, followed by breaking of the bond C6−C6′ (see the next section). We localized the transition state TS1P which separates the reactant and intermediate structure INTP. The C5−C5′ distance in TS1P is calculated as 2.021 Å (Table 2). The C5′−C4′ distance decreases noticeably from 1.484 Å in the dimer $U<>U^-$ to 1.390 Å in TS1P, indicative of the formation of a double bond between these atoms. Finally, the cyclobutane-type ring is modified as shown by the change of the dihedral angle C6′−C5′−C5−C6 from −16.4° in PDA to 13.9° in TS1P.

In the intermediate INTP (Figure 2), the distance C5−C5′ is 3.07 Å. During the C5−C5′ splitting process the heterocyclic rings rotate relative to each other around the C6−C6′ bond: the dihedral angle C6′−C5′−C5−C6 reaches −35.1° in INTP (Table 2). The cleavage of the C5−C5′ bond is also connected with spin transfer from center C4′ to center C5. Concomitantly, the C5′−C4′ bond, almost a single bond in the reactant (1.484 Å), shortens to 1.340 Å (Table 2). In the second reaction step, INTP transforms into the products, i.e., to uracil and the corresponding radical. This cleavage proceeds via transition state TS2P (Figure 2) where the bond C6−C6′ is elongated by 0.47 Å relative to its value in the intermediate. Also, the distances C5−C6 and C5′−C6′ shorten considerably in both heterocyclic rings on the way to the transition state TS2P (see Table 2).

The splitting reaction of the deprotonated dimer cation DDC is also shown in Figure 2. The unpaired electron of the reactant is localized at center N3′; the Mulliken spin density of this atom is 0.84. Ring 1′ which is almost planar in the parent system $U<>U^+$ puckers upon deprotonation at N3′ because the hybridization of center N3′ changes from sp[2] to sp[3] (see Figure 2). These changes result in a reduced repulsive interaction between the unpaired electron at center N3′ and the electron lone pairs at the carbonyl oxygen atoms O2′ and O4′; conse-
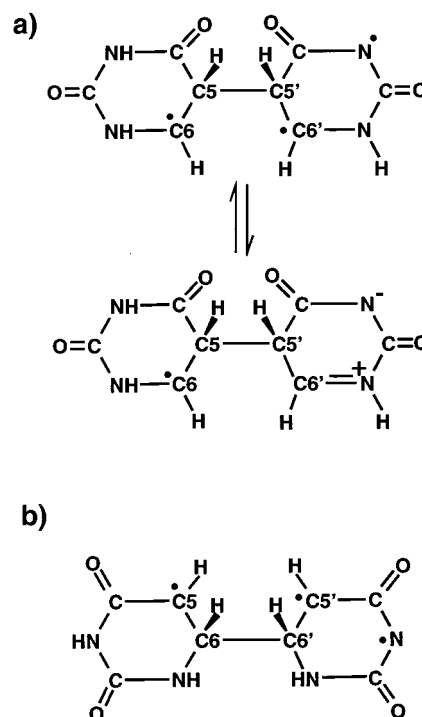


**Figure 3.** Valence structures related to the cleavage of the first bond in DDC: (a) splitting of the bond C6−C6′; (b) splitting of the bond C5−C5′.

quently, deprotonation of $U<>U^+$ is accompanied by a change of the dihedral angle N3′−C4′−O4′−O2′ from −3.1° to −34.1° (Table 3).

The stepwise cycloreversion of DDC proceeds via initial C6−C6′ bond cleavage followed by a splitting of the C5−C5′ bond. The located transition state TS1D which corresponds to the cleavage of the C6−C6′ bond is shown in Figure 2. In TS1D the C6−C6′ distance has increased by 0.51 Å relative to the value in DDC (Table 3). During this reaction step, the dihedral angle C6′−C5′−C5−C6 changes from −20.1° to −14.9°. Furthermore, the C6′−N1′ bond length decreases significantly, from 1.45 Å in DDC to 1.33 Å in TS1D, suggesting a change toward a C=N double bond. Concomitantly, ring 1′ becomes almost planar as indicated by the value of the dihedral angle N3′−C4′−O4′−O2′ in TS1D, 9.0° (Table 3).

The structure of the intermediate species INTD which is formed after cleavage of the C6−C6′ bond (Figure 2) exhibits a very long C6−C6′ distance, 3.39 Å. This elongation is accompanied by a mutual rotation of the heterocyclic rings around the C5−C5′ bond. Correspondingly, the dihedral angle C6′−C5′−C5−C6 changes from −14.9° in TS1D to −91.2° in INTD. The change in the dihedral angle H6′−C6′−N1′−C5′ indicates sp[2] hybridization of the center C6′ while the C6′−N1′ bond undergoes a further shortening, to 1.282 Å (Table 3). In INTD, the unpaired electron is located at the other (non-primed) ring, at center C6. All of these changes reveal a distinctive contribution of a zwitterion resonance structure (Figure 3a) to the electronic state of INTD. In the final reaction step, INTD splits into uracil and a uracil radical species devoid of the hydrogen atom H3′. We found a transition state TS2D of this transformation (Figure 2) where the C5−C5′ bond is elongated by 0.46 Å compared to INTD (Table 3).

To complete this discussion, we would like to comment on the structures obtained by the AM1 method (not shown in Tables 2 and 3). In general, AM1 predicts the correct structural characteristics for the systems under study. The average absolute

Computational Analysis of Proton Transfer

*J. Phys. Chem. A, Vol. 103, No. 18, 1999* **3573**

**TABLE 4: Reaction Energies ΔE for PDA and DDC Calculated in the Gas Phase and in Aqueous Solution (in kcal/mol)**

| | | PDA | | DDC | |
|---|---|---|---|---|---|
| | method | gas phase | water[a] | gas phase | water[a] |
| $\Delta E_1$[b] | B3LYP | −0.2 | −1.6 | −0.9 | −13.1 |
| | AM1 | 11.4 | 9.9 | −7.5 | −19.7 |
| $\Delta E_2$ | B3LYP | −6.3 | −7.8 | −6.7 | 5.7 |
| | AM1 | −10.6 | −12.1 | 10.6 | 23.0 |
| $\Delta E_{tot}$ | B3LYP | −6.5 | −9.5 | −7.6 | −7.4 |
| | AM1 | 0.8 | −2.2 | 3.1 | 3.3 |

[a] Solvent effect on B3LYP results estimated from the corresponding AM1 data. [b] $\Delta E_1$, splitting of the first, C−C bond (C5−C5′ in PDA, C6−C6′ in DDC); $\Delta E_2$, splitting of the second bond; $\Delta E_{tot}$, total process.

**TABLE 5: Activation Barriers $\Delta E^{\neq}$ for the Splitting of PDA and DDC Calculated in the Gas Phase and in Aqueous Solution (in kcal/mol)**

| | | PDA | | DDC | |
|---|---|---|---|---|---|
| | method | gas phase | water[a] | gas phase | water[a] |
| $\Delta E^{\neq}_1$[b] | B3LYP | 10.6 | 10.2 | 13.8 | −1.7 |
| | AM1 | 22.8 | 22.4 | 20.7 | 5.2 |
| $\Delta E^{\neq}_2$ | B3LYP | 8.3 | 6.2 | 9.7 | 6.2 |
| | AM1 | 12.9 | 10.8 | 25.2 | 21.7 |
| $\Delta E^{\neq}_{alt}$ | B3LYP | >47.0 | >47.0 | >41.0 | >40.0 |
| | AM1 | 20.5 | 20.5 | 36.0 | 35.3 |

[a] Solvent effect on B3LYP results estimated from the corresponding AM1 data. [b] $\Delta E^{\neq}_1$, activation energy for the first step (C6−C6′ bond splitting in DDC, C5−C5′ bond splitting in PDA); $\Delta E^{\neq}_2$, splitting of the second bond; $\Delta E^{\neq}_{alt}$, activation energy for the first step along the alternative pathway (C5−C5′ bond splitting in DDC, C6−C6′ bond splitting in PDA).

deviations between bond lengths calculated with AM1 and B3LYP/6-31G* are about 0.03 Å. The AM1 method does not yield a puckered structure for the cyclobutane-type ring as described earlier.[10] For most of the dihedral angles compiled in Tables 2 and 3, the differences of the values calculated by AM1 and B3LYP/6-31G* do not exceed 3°. Thus, the structures computed by AM1 are in reasonable agreement with the B3LYP/6-31G* results.

**Thermodynamic and Kinetic Stability of Protonated U<>U⁻ and Deprotonated U<>U⁺.** A comparison of thermodynamic and kinetic characteristics of the splitting of PDA and DDC with the parameters of the pyrimidine dimer ions will permit us to analyze the influence of protonation or deprotonation on the cycloreversion reaction of the photodimers. The calculated reaction energies and barriers for the cycloreversion of PDA and DDC are collected in Tables 4 and 5.

We start by discussing the B3LYP results for PDA (with solvent effect corrections at the AM1 level). The first step of the splitting of PDA which leads to the intermediate INT1P is slightly exothermic in the gas phase; in a polar environment the reaction becomes more exothermic, by 1.4 kcal/mol, because the dipole moment of the intermediate (6.5 D) is somewhat larger than that of the reactant (5.5 D). The activation barrier of 10.6 kcal/mol calculated for the splitting of the C5−C5′ bond is hardly affected by a polar solvent (Table 5). Note that the first step of the nonconcerted dissociation of U<>U⁻ is associated with a distinctly smaller barrier: 3.9 kcal/mol[10] (by using AM1) or no barrier at all (at the MP2 level[11]). Therefore, PDA is expected to split slower than the corresponding nonprotonated anion.

We also investigated the alternative mechanism of PDA splitting which starts with C6−C6′ bond cleavage. However,
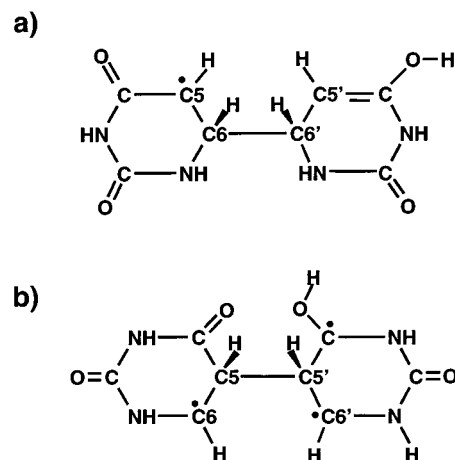
**Figure 4.** Valence structures related to the cleavage of the first bond in PDA: (a) splitting of the bond C5−C5′; (b) splitting of the bond C6−C6′.

because of convergence problems we were unable to locate the transition state of this process. Instead, a sequence of constrained geometry optimizations was carried out with the C6−C6′ distance increasing in stepwise fashion. This approach allowed us to estimate the kinetic barrier to be higher than 47 kcal/mol (see $\Delta E^{\neq}_{alt}$ in Table 5). Thus, the opening of the PDA ring is initiated by C5−C5′ bond splitting, followed by the cleavage of the C6−C6′ bond. Figure 4 shows valence structures describing either type of splitting. For the "normal" pathway (where the C5−C5′ bond splits first), a structure results which is stabilized by the double bond C4′=C5′ and where the spin is localized at center C5. By contrast, formation of a stabilizing double bond is impossible after initial C6−C6′ bond splitting (Figure 4b). This finding may be invoked to rationalize the calculated difference in the barriers. Note that AM1 predicts the activation energies to be similar for "normal" and alternative pathways of the PDA splitting (see Table 5).

The second step of the splitting reaction of PDA, the decay of INTP, is calculated to be exothermic both in the gas phase, by −6.3 kcal/mol, and in aqueous solution, by −7.8 kcal/mol (Table 4); the corresponding values of the activation barrier are 8.3 and 6.2 kcal/mol, respectively. Again, the larger dipole moment of TS1P (as compared to INTP) is responsible for the lower barrier in a polar medium. Thus, while the total splitting is calculated to be exothermic by −6.5 kcal/mol in the gas phase and by −9.5 kcal/mol in aqueous solution (Table 4), activation barriers impede the process.

The splitting of DDC starts with a dissociation of the C6−C6′ bond which is slightly exothermic in the gas phase, −0.9 kcal/mol (Table 4). However, the solvation effect is quite different from that of PDA: the reaction energy of DDC becomes more exothermic in aqueous solution, −12.2 kcal/mol (Table 4). This strong environmental effect can be rationalized by a substantial charge separation in the zwitterion-like intermediate INTD (Figure 3a). Because of the charge separation in the transition state TS1P, the activation barrier in the gas phase, 13.8 kcal/mol, completely disappears in aqueous solution; the corresponding solvent effect is estimated to be −15.5 kcal/mol (Table 5). Thus, requiring noticeable activation in the gas phase, DDC splitting is calculated to occur spontaneously in aqueous solution. This finding correlates well with the experimentally observed quantitative repair of DNA by rhodium(III) complexes[6] or model reaction in the solutions.[15]

The activation barrier along the alternative reaction path, where the splitting of DDC starts with the cleavage of the C5−

C5′ bond, is estimated to be higher than 40 kcal/mol (Table 5). Again, this result is based on calculations of an approximate reaction coordinate. The difference in the barriers for the initial splitting of the C5−C5′ and C6−C6′ bonds can be rationalized as follows. Unlike the cleavage of the C6−C6′ bond, the splitting of the C5−C5′ bond results in a valence structure with spin localized at the centers N3′, C5, and C5′. Lack of resonance stabilization in the transition state as well as in the intermediate leads to a much higher barrier for C5−C5′ splitting than for C6−C6′ cleavage. For DDC, the predictions of AM1 are in qualitative agreement with the B3LYP results.

The intermediate INTD dissociates by forming a uracil molecule and a uracil radical species (actually, a uracil devoid of H3′). This transformation is exothermic in the gas phase, −6.7 kcal/mol. However, in aqueous solution one observes a strong endothermic solvent effect of 12.5 kcal/mol (Table 4) connected with the polar structure of INTD. The corresponding transition state TS2D (Figure 2) exhibits an activation barrier of 9.7 kcal/mol which is lowered to 6.2 kcal/mol in aqueous solution (Table 5). This barrier in solution is easily overcome at ambient temperatures. AM1 overestimates the activation energy $\Delta E^{\neq}_2$ (Table 5).

The splitting of DDC is an exothermic transformation with the reaction energy hardly affected by solvent effects (0.2 kcal/mol; Table 4). However, unlike PDA, DDC splits in water without any (or with a rather small) activation barrier. Thus, deprotonation of the dimer cation does not prevent its splitting.

## Conclusions

We have investigated the role of protonation/deprotonation on the splitting reaction of pyrimidine dimer ions. This problem is of interest for the repair of DNA which may occur via two pathways, (i) in vivo due to photoreduction of the photodimer by a flavoenzyme of the photolyase type and (ii) in vitro in the presence of photoreducing sensitizers as well as as the result of oxidative splitting initiated by an exogenous oxidant attached to oligonucleotides.

**The Dimer Anion Py<>Py⁻.** The present study suggests that protonation of the dimer anion due to proton transfer from a complementary adenine in DNA is energetically unfavorable, similar to the previous experimental[16,17] and computational findings.[32] However, other proton donors stronger than adenine may well protonate the dimer anion.

The activation barrier for the splitting of the C5−C5′ bond in the dimer anion is negligible in contrast to its protonated state. In the latter case the activation energy is about 10 kcal/mol in both the gas phase and a polar environment. This finding might relate to the experimental observation that the splitting efficiency of pyrimidine dimer anions is much smaller when the reaction proceeds in polar solution, especially at low pH.[9]

**The Dimer Cation Py<>Py⁺.** Unlike the anion Py<>Py⁻, proton transfer from the dimer cation to adenine seems to be favorable in DNA, in accordance with experimental[16] and computational[32] findings for the related system that consists of a thymine cation and adenine. For the splitting of the relevant C6−C6′ bond of a deprotonated dimer cation, a rather high activation barrier is found in the gas phase. This activation energy depends significantly on the environment and disappears in polar solution because of the zwitterion character of the corresponding transition state. Therefore, in aqueous solution the splitting of the deprotonated dimer cation is also predicted to proceed without an essential activation barrier.

In summary, when there is no proton exchange with the dimer environment, opening of the cyclobutane ring of the pyrimidine photodimer is expected to proceed readily, irrespective of whether the dimer carries a positive or negative charge. In DNA, so far only the reductive splitting is realized utilizing a local charge transfer interaction between the flavine cofactor and the photodimer. This exclusively anionic photorepair mechanism might well reflect an evolutionary optimization principle which is aimed at avoidance of high power oxidants in biological tissue.

**References and Notes**

(1) Jeffrey, A. G.; Sänger W. *Hydrogen Bonding in Biological Structures*; Springer: New York, 1991.

(2) Jeffrey, A. G. *An Introduction to Hydrogen Bonding*; Oxford University Press: New York, 1997.

(3) Scheiner S. *Hydrogen Bonding. A Theoretical Perspective*. Oxford University Press: New York, 1997.

(4) Fersht, A. *Enzyme Structure and Mechanism*; Freeman: New York, 1985.

(5) Kim S.-T.; Sancar, A. *Photochem. Photobiol.* **1993**, *57*, 895.

(6) Dandliker, P. J.; Holmlin, R. E.; Barton, J. K. *Science* **1997**, *275*, 1465.

(7) Begley, T. P. *Acc. Chem. Res.* **1994**, *27*, 394.

(8) Pouwels, P. J. W.; Hartman, R. F.; Rose, S. D.; Kaptein, R. *Photochem. Photobiol.* **1995**, *61*, 563; 575.

(9) Epple, R.; Wallenborn, E.-U.; Carell, T. *J. Am. Chem. Soc.* **1997**, *119*, 7440.

(10) Voityuk, A. A.; Michel-Beyerle, M.-E.; Rösch, N. *J. Am. Chem. Soc.* **1996**, *118*, 9750.

(11) Voityuk, A. A.; Röch, N. *J. Phys. Chem. A* **1997**, *101*, 8335.

(12) Aida, M.; Inoue, F.; Kaneko, M.; Dupuis, M. *J. Am. Chem. Soc.* **1997**, *119*, 12274.

(13) Rak, J.; Voityuk, A. A.; Rösch, N. *J. Phys. Chem. A* **1998**, *102*, 7168.

(14) Rak, J.; Voityuk, A. A.; Rösch, N. *J. Mol. Struct. (THEOCHEM)* **1999**, in press.

(15) Heelis, P. F.; Kim, S.-T.; Okamura, T.; Sancar, A. *J. Photochem. Photobiol. B: Biol.* **1993**, *17*, 219.

(16) Steenken, S. *Chem. Rev.* **1989**, *89*, 503.

(17) Steenken, S.; Telo, J. P.; Novais, H. M.; Candeias, L. P. **1992**, *114*, 4701.

(18) *Gaussian 94*, Revision D.4, Frisch, M. J.; Trucks, G. W.; Schlegel, H. B.; Gill, P. M. W.; Johnson, B. G.; Robb, M. A.; Cheeseman, J. R.; Keith, T.; Petersson, G. A.; Montgomery, J. A.; Raghavachari, K.; Al-Laham, M. A.; Zakrzewski, V. G.; Ortiz, J. V.; Foresman, J. B.; Cioslowski, J.; Stefanov, B. B.; Nanayakkara, A.; Challacombe, M.; Peng, C. Y.; Ayala, P. Y.; Chen, W.; Wong, W. M.; Andres, J. L.; Replogle, E. S.; Gomperts, R.; Martin, R. L.; Fox, D. J.; Binkley, J. S.; Defrees, D. J.; Baker, J.; Stewart, J. J. P.; Head-Gordon, M.; Gonzalez, C.; Pople, J. A. Gaussian: Pittsburgh, 1995.

(19) Dewar, M. J. S.; Zoebisch, E. G.; Healy, E. F.; Stewart, J. J. P. *J. Am. Chem. Soc.* **1985**, *107*, 3902.

(20) Voityuk, A. A. *SIBIQ 2.4. A Program for Semiempirical Calculations*, 1995.

(21) Hariharan, P. C.; Pople, J. A. *Theor. Chim. Acta* **1973**, *28*, 213.

(22) Becke, A. D. *Phys. Rev. A* **1988**, *37*, 785.

(23) Becke, A. D. *J. Chem. Phys.* **1993**, *98*, 5648.

(24) Lee, C.; Yang, W.; Parr, R. G. *Phys. Rev. B* **1988**, *41*, 785.

(25) Curtiss, L. A.; Raghavachari, K.; Redfern, P. C.; Pople, J. A. *J. Chem. Phys.* **1997**, *106*, 1063.

(26) Bally, T.; Sastry, G. N. *J. Phys. Chem. A* **1997**, *101*, 7923.

(27) Zhang, Y.; Yang, W. *J. Chem. Phys.* **1998**, *107*, 2604.

(28) Hehre, W. J.; Radom, L.; Schleyer, P. v. R.; Pople, J. A. *Ab initio Molecular Orbital Theory*, Wiley: New York, 1986.

(29) Tomasi, J.; Persico, M. *Chem. Rev.* **1994**, *94*, 2027−2094.

(30) Adman, E.; Gordon, M. P.; Jensen, L. H. *J. Chem. Soc., Chem. Commun.* **1968**, 1019.

(31) Camerman, N.; Camerman, A. *J. Am. Chem. Soc.* **1970**, *92*, 2523.

(32) Colson, A.-O.; Besler, B.; Sevilla, D. *J. Phys. Chem.* **1992**, *96*, 9787.